Journal of Steroid Biochemistry and Molecular Biology 211 (2021) 105907

Contents lists available at ScienceDirect

Journal of Steroid Biochemistry and Molecular Biology

journal homepage: www.elsevier.com/locate/jsbmb

Vitamin D receptor and 1α-hydroxylase are highly expressed in lungs of mice infected with H9N2 avian influenza viruses

Pengjing Lian [a], Yu Bai [a], Jingyun Li [a], Hongyan Wang [b], Xiaofei Niu [b], Zihui Zhang [a], Hongru Li [a], Lihong Zhao [a], Jian Qiao [a,*]

[a] Department of Pathophysiology, College of Veterinary Medicine, China Agricultural University, Beijing, China
[b] Department of Veterinary Medicine, College of Life Sciences and Food Engineering, Hebei University of Engineering, Handan, China

ARTICLE INFO

Keywords:
Vitamin D
H9N2 avian influenza virus
1α-Hydroxylase
Vitamin D receptor
24-Hydroxylase
Mice

ABSTRACT

The H9N2 avian influenza viruses infect poultry worldwide, and can potentially cause a human pandemic without adaptation. Vitamin D3 (D3) is increasingly being recognized for its extra-skeletal roles, such as the inflammatory and immune responses to infection. The aim of this study was to analyze the changes in vitamin D metabolizing enzymes and vitamin D receptor (VDR) in the lung tissues of mice infected with H9N2. The mice were intranasally inoculated with the appropriate dose of the virus, and various clinical indices were measured on days 3, 7, 14 and 21 post-infection. H9N2 infection significantly increased the expression levels of 1α-hydroxylase mRNA and protein, which is the activating enzyme of 25-hydroxyvitamin D ($25(OH)D_3$), but had no significant effect on the $25(OH)D_3$ inactivating enzyme 24-hydroxylase, indicating that inactive D3 might be converted to its active form in the H9N2-infected lungs. Furthermore, a significant increase was also observed in the VDR mRNA and protein levels, suggesting enhanced responsiveness of the lung tissues to 1, $25(OH)_2D_3$ post H9N2 infection. In addition, daily $25(OH)D_3$ injection from day 2–14 post-infection did not affect the clinical signs, virus replication and cytokine (IL-1β and TNF-α) production in the lungs of the infected mice. Given that the biological effects of D3 rely on its activation, and the binding of 1, $25(OH)_2D_3$ to VDR in specific tissues, our findings provide novel insights into the possible role of vitamin D in the development and progression of influenza.

1. Introduction

H9N2 avian influenza viruses are highly prevalent in poultry farms worldwide, and have caused considerable economic losses [1]. H9N2 viruses have been isolated from pigs with influenza-like symptoms in Mainland China since 1998 [2], and an avian origin H9N2 influenza virus was recently isolated from dogs in Southern China [3]. Occasional cases of H9N2 infection in humans have also been reported in China [4–6], and some H9N2 viruses currently circulating in birds display human influenza virus-like receptor specificity [7]. These findings indicate that H9N2 viruses can cross species barriers and expand their host range from poultry to humans and other mammals, and are therefore considered most likely to cause a new influenza pandemic in humans [8]. In addition, H9N2 is the gene donor for other influenza viruses, including H5N1, H7N9, H10N8 and H5N6 [9–12]. Therefore, H9N2 virus has posed a great threat to public health.

In recent decades, the association between vitamin D3 (D3) and influenza has aroused great interest. Hope-Simpson assumed that the seasonal pattern of influenza infection correlates with the seasonal serum D3 levels [13,14]. Since D3 is primarily produced in the skin during sun exposure as opposed to absorption from dietary sources, its circulating levels are lower in winter due to fewer hours of sunlight [15,16]. Moan et al. compared the seasonal pattern of influenza and pneumonia-related deaths to that of serum D3 levels in Norway during a 30-year period from 1980 to 2000, and observed significantly higher mortality rate in the winters that corresponded to lower D3 serum levels [17]. Although model simulations of the seasonal fluctuation of D3 did not consistently reproduce the observed seasonal patterns of influenza [18], it is possible that D3 might play a protective role during influenza infection.

Vitamin D3 regulates calcium and phosphorus metabolism, and is a crucial factor in bone-formation [19]. However, the vitamin D receptor (VDR) and vitamin D activating enzymes are expressed in cell types other than those involved in mineral and bone homeostasis, which

* Corresponding author at: Department of Pathophysiology, College of Veterinary Medicine, China Agricultural University, Beijing, 100193, China.
E-mail address: qiaojian@cau.edu.cn (J. Qiao).

https://doi.org/10.1016/j.jsbmb.2021.105907
Received 23 February 2021; Received in revised form 21 April 2021; Accepted 3 May 2021
Available online 10 May 2021

strongly indicates a more diverse role for D3 than originally established. Indeed, activation of VDR has non-classical effects [20], such as innate and adaptive immune responses [21]. For example, 1, 25-dihydroxyvitamin D_3 (1, $25(OH)_2D_3$), the bioactive metabolite of D3, upregulates antimicrobial peptides such as cathelicidin LL-37 and beta defensin 2 in the macrophages and monocytes *in vitro* [22,23]. In addition, both 1, 25 $(OH)_2D_3$ and a vitamin D analogue decreased *in vitro* proinflammatory cytokine and chemokine production in infected human respiratory epithelial cells [24,25].

The immunomodulatory effects of D3 rely on the activation of 25-hydroxyvitamin D ($25(OH)D_3$) in specific tissues, which is then converted by 1α-hydroxylase to 1, $25(OH)_2D_3$, the high-affinity VDR ligand that subsequently modulates the expression of D3 target genes [15]. Recently, a noncanonical pathway of D3 activation involving cytochrome P450 side chain cleavage (P450scc, CYP11A1) was discovered in human and porcine cells [26,27]. In addition, alternative nuclear receptors for CYP11A1-derived D3-hydroxy-derivatives and $1,25(OH)_2D_3$ have also been identified, and include the retinoid-related orphan receptors α and γ [28] and the aryl hydrocarbon receptor [29]. The activity of 1, $25(OH)_2D_3$ is autoregulated *via* induction of 24-hydroxylase, which catalyzes the first step of D3 catabolism and thus prevents excessive D3 signaling [30]. Studies show that human respiratory epithelial cells and various immune cells express 1α-hydroxylase and VDR *in vitro* [21,31]. However, little is known regarding D3 metabolism and VDR expression in the target tissues during influenza infection *in vivo*. In a previous study, we found that the H9N2 virus caused severe lung injury in mice [32]. The aim of the present study was to assess the expression of vitamin D3 metabolic enzymes and VDR in the lung tissues of mice during H9N2 infection. Our results showed that VDR and 1α-hydroxylase were highly expressed in the lungs of the H9N2-infected mice, which provides novel mechanistic insights into the association between vitamin D and influenza.

2. Materials and methods

2.1. Virus propagation

The H9N2 virus was isolated from chickens in Hebei province, China and was designated as A/Chicken/Hebei/4/2008 (H9N2) (Ck/HB/4/08). The complete genome sequences of the virus are available in the GenBank database under accession numbers FJ499463–FJ499470 [33]. The viruses were propagated in the allantoic cavity of 10-days-old SPF embryonated eggs for 72 h at 37℃, and the allantoic fluid was centrifuged and stored at −80℃. The virus titers were measured in terms of the median tissue culture infectious dose ($TCID_{50}$) as described previously [34].

2.2. Mouse infection and treatment

Specific-pathogen-free (SPF) BALB/c male mice (aged 6–8 weeks and weighing 20 g) were purchased from Beijing Vital River Laboratory Animal Technology Co. Ltd. (China). The animals were maintained according to the National Institutes of Health (NIH) standards established in the Guidelines for the Care and Use of Experimental Animals, and all experimental protocols were reviewed and approved by the Animal Investigation Committee of China Agricultural University.

The mice were randomly divided into the infected and non-infected groups (n = 30 each), lightly anaesthetized with isoflurane, and inoculated intranasally (100 μl) with 1×10^6 $TCID_{50}$ H9N2 virus diluted in sterile saline, or the equivalent dilution of non-infectious allantoic fluid. The virus dose was determined on the basis of a pilot experiment. The body weight and activity of mice were monitored daily. Five mice from each group were randomly euthanized on 3, 7, 14 and 21 days post-infection (DPI). The blood was collected *via* enucleation of eyeball and the serum was extracted. The lungs were collected and the lung index was calculated by dividing the lung wet weight with the body weight. Lung gross lesions were assessed on 3 and 7 DPI. The virus titers in the lungs were measured by $TCID_{50}$ assay on 3, 7 and 14 DPI. The tissue samples were preserved for subsequent molecular assays.

To evaluate the effect of $25(OH)D_3$ on viral infection, the mice were randomly divided into the uninfected + saline, uninfected + $25(OH)D_3$, infected + saline and infected + $25(OH)D_3$ groups (Table 1, n = 30 mice/group). All mice were fed a diet supplemented with 41.7 μg/kg D3 for 4 weeks, resulting in a daily intake of 0.12 μg D3. The mice were inoculated with 1×10^6 $TCID_{50}$ H9N2 or non-infectious allantoic fluid as appropriate, and then intraperitoneally injected with 0.2 mL saline or 4 μg/kg $25(OH)D_3$ from 2–14 DPI. The dose of $25(OH)D_3$ was higher than the normal serum level of 30 ng/mL [35]. The body weight and activity of mice were monitored daily, and 5 mice from each group were randomly euthanized on 3, 7, 14 and 21 DPI. Blood samples and lungs were collected for ELISA and histopathological analysis.

2.3. Lung histopathology

The lungs tissues were fixed in buffered 10 % formalin and embedded in paraffin. Four-micrometer-thick sections were cut and stained with hematoxylin-eosin (H&E) as per standard protocols.

2.4. Quantitative real time PCR

The lung tissues collected on 3, 7, 14 and 21 DPI were snap frozen in liquid nitrogen, and homogenized in Trizol reagent. Total RNA was extracted from the homogenates using the TRNzol kit (TIANGEN BIOTECH, Beijing) according to the manufacturer's instructions. One microgram total RNA was reverse transcribed to cDNA using the PrimeScript RT reagent Kit with gDNA Eraser (TaKaRa, RR037A, Japan). Amplification was checked by 1% agarose gel electrophoresis, and the target fragment was purified. The cDNA was cloned into the pMD18-T plasmid, and transformed into DH5a cells. The positive clones were identified by colony PCR and sequencing, and the plasmids were extracted and measured quantified at 260 nm. The number of gene copies were calculated as follows:

Number of copies (copies/μl) = X (g/μL) * 10^{-9} * 6.02 * 10^{23} / (clone size bp *660). Note: X (ng/μL) = OD260 * 50, 6.022×10^{23} = Avogadro number, 660 g/mol = molecular mass of 1 bp dsDNA, clone size bp = plasmid (pMD18-T = 2692bp) + insert (1α-hydroxylase = 278bp, VDR = 325bp, 24-hydroxylase = 154bp).

The plasmid standard was serially diluted 10-fold, and 2 μl of each dilution was used as the template to establish the standard curve. The cDNA was amplified RT-qPCR using Tli RNaseH Plus (SYBR® Premix Ex Taq™ II, TaKaRa, Japan), and gene copy numbers were obtained from the standard curve using the threshold cycle (Ct) values. The primer sequences for 1α-hydroxylase, VDR and 24-hydroxylase were designed and synthesized by Invitrogen (Table 2).

2.5. Western blotting

Proteins were extracted from the lung tissues collected on 3 and 7

Table 1
mouse groups in 25(OH)D treatment experiment.

Group	Primary inoculation	Secondary injection on days 2–14 post- inoculation
Saline-treated infected	H9N2 viruses	0.2 mL sterile saline
$25(OH)D_3$-treated infected	H9N2 viruses	0.2 mL sterile $25(OH)D_3$ solution (4 μg/kg)
Saline-treated uninfected	noninfectious allantoic fluid	0.2 mL sterile saline
$25(OH)D_3$-treated uninfected	noninfectious allantoic fluid	0.2 mL sterile $25(OH)D_3$ solution (4 μg/kg)

Table 2
primer sequence of VDR, 1α-hydroxylase and 24-hydroxylase.

Gene	Forward primer (5'-3')	Reverse primer (5'-3')
VDR	AGCACATTATCGCCATCC	GTACTTACGTCTGCACGAATT
1α-hydroxylase	GACCTTGTGCGACGACTAA	GAGCCCACTGCATGTATGA
24-hydroxylase	GGACCTGCGCCCTAAACAACT	CGGAAGTGCTGTTGGGTTCTGA

DPI using RIPA buffer, and quantified using the BCA assay (Solarbio, PC0020, China). Equal amounts of protein per sample were separated by SDS-polyacrylamide gel electrophoresis, and transferred to polyvinylidene fluoride (PVDF) membranes. The blots were probed with mouse monoclonal anti-VDR antibody (Santa Cruz Biotechnology, sc-13133, USA), mouse monoclonal anti-1α-hydroxylase antibody (Santa Cruz Biotechnology, sc-515903, USA), rabbit polyclonal anti-24-hydroxylase antibody (Abcam Inc., cat#203308, USA) and mouse monoclonal anti-GAPDH antibody (Beyotime, AG019, China), followed by HRP-conjugated secondary antibody. The protein bands were developed using ECL hypersensitive luminous solution (Wan Lei, WLA006, China) and detected using a CCD imaging system. Gray values were measured using Image J. The relative target protein levels were calculated using GAPDH as the internal control.

2.6. ELISA

The 25(OH)D_3 levels in serum were measured using an ELISA kit (MLBIO Biotechnology Co. Ltd, ml038442, Shanghai). The lung tissues were ground, and the homogenates were resuspended in 1 mL sterile PBS and centrifuged on 8000 rpm. The supernatant was collected, and the levels of IL-1β (R&D systems, MLB00C, USA) and TNF-a (R&D systems, MTA00B, USA) were measured using specific kits according to the manufacturer's instructions.

2.7. $TCID_{50}$ assay for virus titer

Virus titers were measured as described previously [34] using the Madin–Darby canine kidney cell (MDCK) line (Beijing University of Agriculture). The supernatants of the lung homogenates were filtered through a 200 nm membrane, and used to infect the MDCK cells cultured in Dulbecco's Modified Eagle Medium (DMEM; HyClone) supplemented with 10 % fetal bovine serum (FBS; Gibco) and 1% penicillin-streptomycin (Gibco) at 37 °C under 5% CO_2. Virus titers were expressed as mean $\log_{10}$ $TCID_{50}$ per milliliter ± standard deviation.

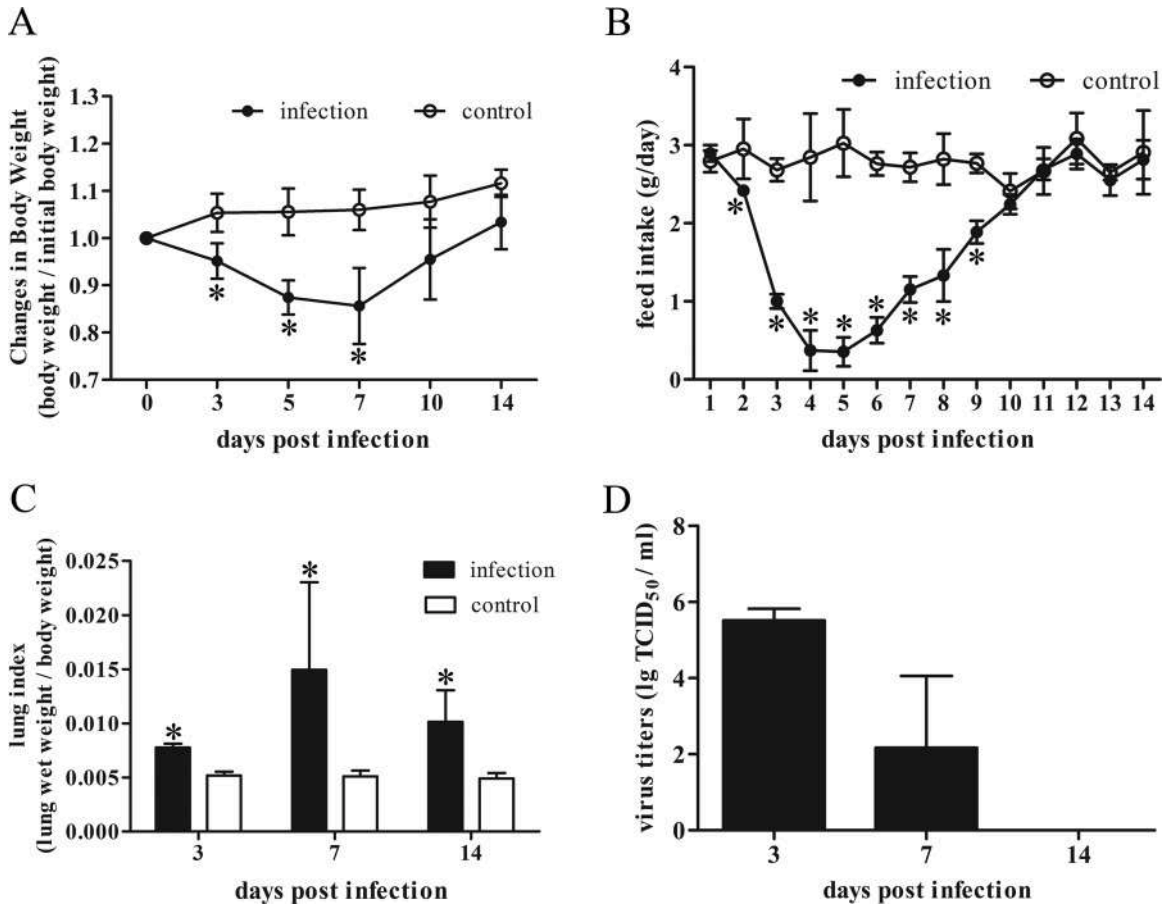

Fig. 1. The clinical signs, lung indexes and vital titers after H9N2 viral infection in mice. Infected mice and control mice were intranasally inoculated with 1×10^6 $TCID_{50}$ of H9N2 viruses, or noninfectious allantoic fluid, respectively. (A) The body weight changes of infected and control mice. (B) The feed intake of infected and control mice. (C) The lung indexes of infected and control mice on days 3, 7 and 14. (D) Replication of H9N2 viruses in lungs of infected mice. The feed intake was determined by measuring food weight loss per group and dividing by number of mice. The data of feed intake were from three repeated experiments and were presented as mean ± SD (n = 3). The data of body weight, lung indexes and viral titers were presented as mean ± SD (n = 5) *: $P < 0.05$ compared with control mice.

2.8. Statistical analysis

All data were analyzed using the SPSS software (version 20). All data except that of the feed intake are shown as the mean ± SD. The Student's *t* test was used to compare different groups. *P*-values less than 0.05 were considered statistically significant.

3. Results

3.1. H9N2 causes acute respiratory disease in BALB/c mice

The mice infected with H9N2 presented a relatively acute clinical disease. The animals exhibited weight loss (Fig. 1A), lack of appetite (Fig. 1B), inactivity and ruffled fur at 3 DPI, and progressed to severe symptoms including labored respiration, complete appetite loss, emaciation and 13.5 % weight loss by day 7. The lungs of the infected mice were highly edematous with profuse hemorrhagic areas, and the lung indices (Fig. 1C) were markedly elevated on day 3 and peaked to nearly 4-fold higher compared to that of the control mice on day 7. High virus titers were observed in the lungs of the infected mice on day 3 (Fig. 1D), which dropped on day 7 and were undetectable on day 14. Consistent with this, the mice gradually recovered and regained their weight by 14 DPI. Taken together, the H9N2 virus causes acute respiratory disease in BALB/c mice.

3.2. H9N2 infection affects vitamin D3 metabolism and activity

The conversion of 25(OH)D_3 into its active form 1, 25$(OH)_2D_3$ is catalyzed by 1α-hydroxylase. As shown on Fig. 2, 1α-hydroxylase mRNA levels increased slightly in the lungs of infected mice on 3 DPI, and were elevated almost 5-fold compared to the non-infected controls on day 7, before decreasing to baseline levels on days 14 and 21. Consistent with this, the infected mice exhibited a significant increase in 1α-hydroxylase protein expression in their lungs on days 3 and 7 (Fig. 3A, B), and the increase was 4-fold compared to the non-infected controls on day 7. These results indicated that the inactive D3 might be converted to the active form in the lung tissues during H9N2 infection.

The biological effects of 1, 25$(OH)_2D_3$ are mediated *via* VDR signaling. As shown in Fig. 4, the pulmonary VDR mRNA levels were unaffected on day 3 post-infection but increased significantly compared to the uninfected controls on days 7 and 14. VDR protein levels on the other hand were upregulated almost 4-fold compared to the control mice

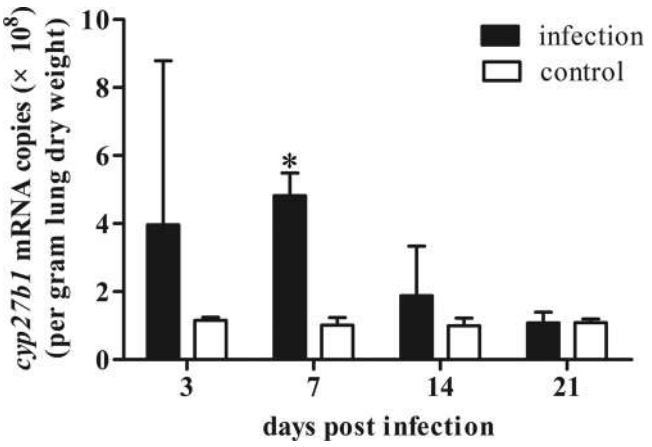

Fig. 2. The *1α-hydroxylase* mRNA (*cyp27b1* mRNA) expression levels in lungs of mice after infection. Mice were infected with 1 × 10^6 $TCID_{50}$ of H9N2 viruses and the lung tissues were collected on days 3, 7, 14 and 21 post-infection. Absolute RT-qPCR assay was used to measure the expression of *cyp27b1* mRNA. The data are expressed as mean ± SD (n = 5). *: $P < 0.05$ compared with control group.

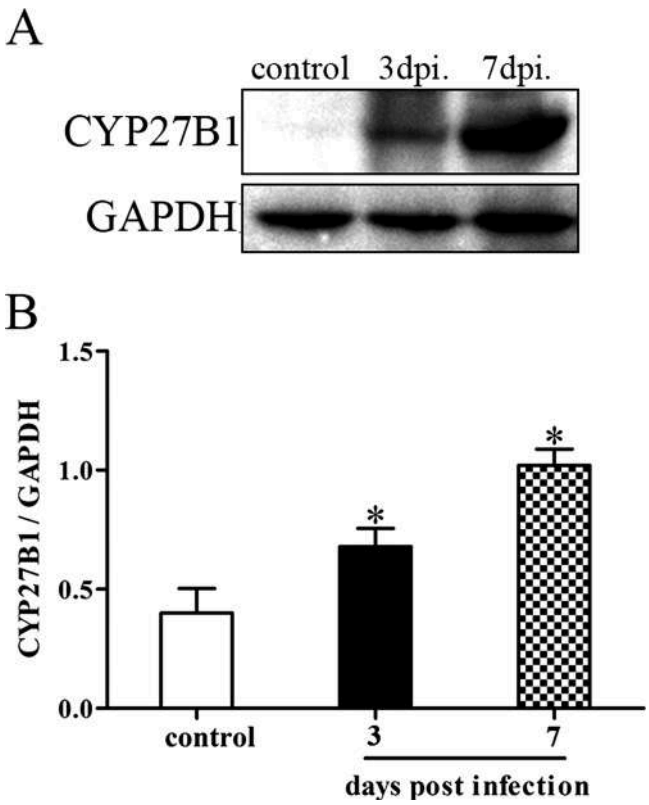

Fig. 3. The protein expression levels of 1α-hydroxylase (CYP27B1) in lungs of mice after infection. Mice were infected with 1 × 10^6 $TCID_{50}$ of H9N2 viruses and the lung tissues were collected on days 3 and 7 post-infection. Western boltting assay was used to measure the protein expression of CYP27B1. Fig. A was electrophoretic image and Fig. B was the data of CYP27B1 protein relative expression to GAPDH. The data are expressed as mean ± SD (n = 5). *: $P < 0.05$ compared with control mice. dpi., days post infection.

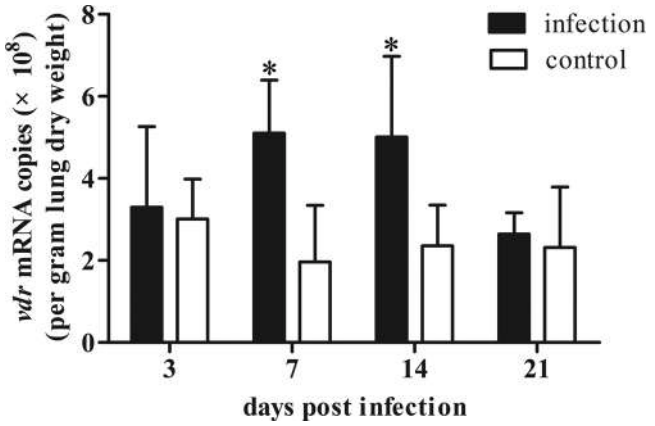

Fig. 4. The *vdr* mRNA expression levels in lungs of mice after infection. Mice were infected with 1 × 10^6 $TCID_{50}$ of H9N2 viruses and the lung tissues were collected on days 3, 7, 14 and 21 post-infection. Absolute RT-qPCR assay was used to measure the expression of *vdr* mRNA. The data are expressed as mean ± SD (n = 5). *: $P < 0.05$ compared with control group.

on days 3 and 7 post-infection (Fig. 5A, B). These results indicated that H9N2 may enhance the responsiveness of lung tissues to 1, 25$(OH)_2D_3$.

The conversion of 25(OH)D_3 and 1, 25$(OH)_2D_3$ to 24-hydroxylated intermediates by 24-hydroxylase is necessary for further catabolism. However, H9N2 infection had no discernible effect on the 24-hydroxylase mRNA levels at the different time points (Fig. 6), whereas the 24-

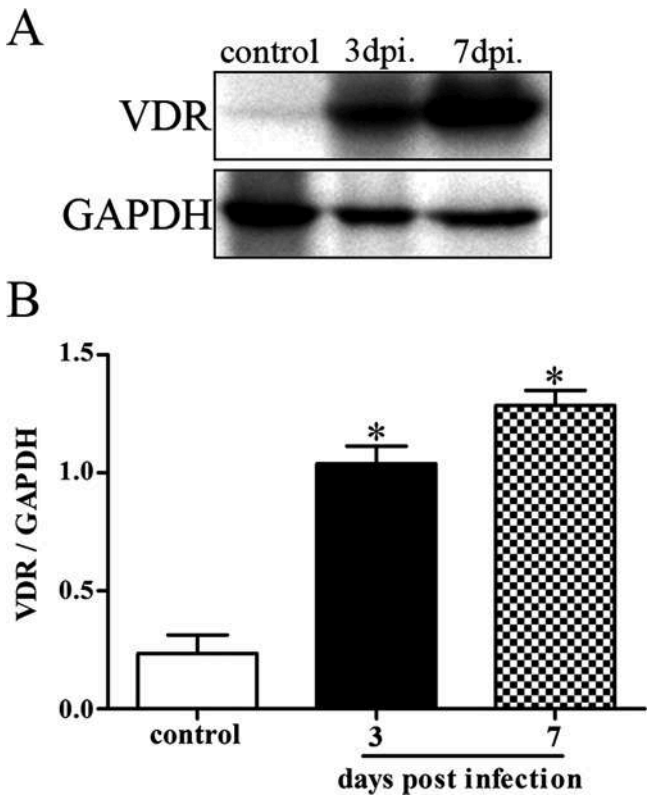

Fig. 5. The protein expression levels of VDR in lungs of mice after infection. Mice were infected with 1 × 10^6 $TCID_{50}$ of H9N2 viruses and the lung tissues were collected on days 3 and 7 post-infection. Western boltting assay was used to measure the expression of VDR protein. Fig. A was electrophoretic image and Fig. B was the data of VDR protein relative expression to GAPDH. The data are expressed as mean ± SEM (n = 5). *: $P < 0.05$ compared with control mice. dpi., days post infection.

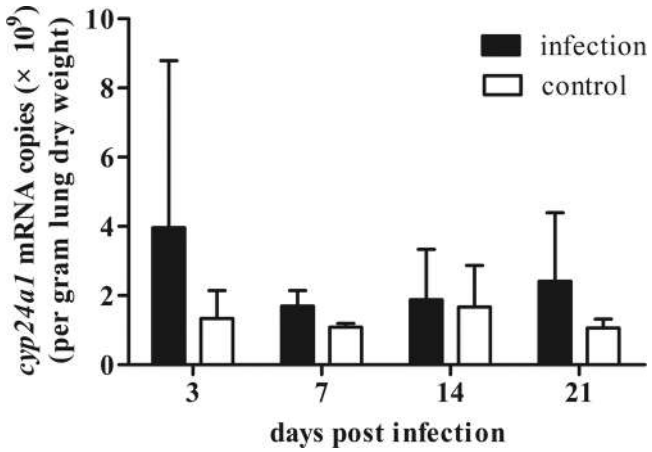

Fig. 6. The *24-hydroxylase* mRNA (*cyp24a1* mRNA) expression levels in lungs of mice after infection. Mice were infected with 1 × 10^6 $TCID_{50}$ of H9N2 viruses and the lung tissues were collected on days 3, 7, 14 and 21 post-infection. Absolute RT-qPCR was used to measure the expression of *cyp24a1* mRNA. The data are expressed as mean ± SD (n = 5).

hydroxylase protein was expressed at low levels in the lungs of both the infected and control mice (Fig. 7A, B). Taken together, H9N2 most likely activates D3 and VDR-dependent downstream signaling without affecting its metabolism.

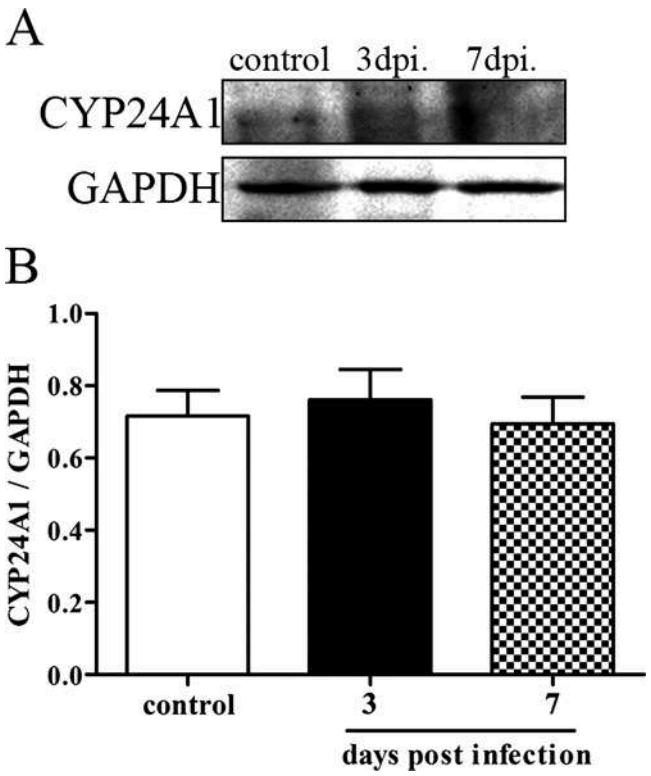

Fig. 7. The protein expression levels of 24-hydroxylase (CYP24A1) in lungs of mice after infection. Mice were infected with 1 × 10^6 $TCID_{50}$ of H9N2 viruses and the lung tissues were collected on days 3 and 7 post-infection. Western bolt assay was used to measure the expression of CYP24A1 protein. Fig. A was electrophoretic image and Fig. B was the data of CYP24A1 protein relative expression to GAPDH. The data are expressed as mean ± SD (n = 5). dpi., days post infection.

3.3. 25(OH)D treatment had little effect on H9N2 infection

The significant upregulation of 1α-hydroxylase and VDR in the lungs of H9N2-infected mice suggested a potential therapeutic effect of D3. Therefore, we treated the mice with 25(OH)D_3 over a period of 14 days after H9N2 infection. Although 25(OH)D_3 supplementation significantly increased serum 25(OH)D_3 levels on days 7 and 14 (Fig. 8), it had little

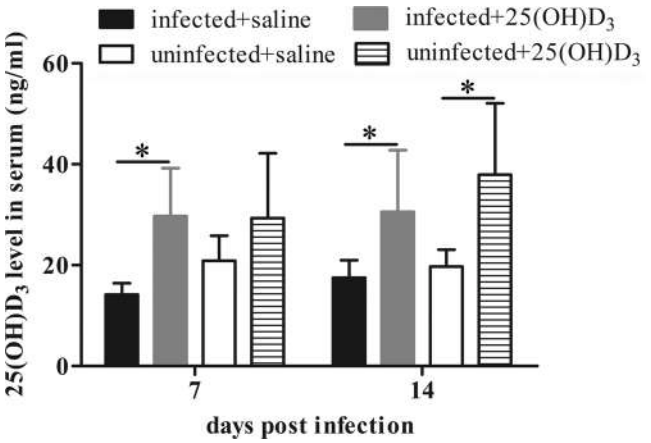

Fig. 8. Serum 25(OH)D_3 level after 25(OH)D_3 treatment. Mice were intranasally inoculated with H9N2 viruses, and then were intraperitoneally injected daily with 0.2 mL 25(OH)D_3 solution (4 μg/kg) on days 2 to 14 post-infection. The bloods were collected on days 7 and 14. Serum 25(OH)D_3 levels were measured by ELISA and the data were presented as mean ± SD (n = 5). *: $P < 0.05$.

effect on clinical signs such weight loss (Fig. 9A) and inactivity compared to the saline-treated infected mice. In addition, the lung indices were also similar in the 25(OH)D_3-treated and saline-treated infected mice at the different time points post-infection (Fig. 9B). As shown in Fig. 10A, both groups exhibited similar extent of edema and hemorrhage on day 7 post-infection, and all H9N2-infected mice had severe interstitial and alveolar edema, hemorrhage, alveolar wall thickening and inflammatory cell infiltration in the lungs (Fig. 10B). The H9N2 titers were measured on days 3 and 7 post-infection, and were not significantly different between the 25(OH)D_3-treated and saline-treated infected mice (Fig. 11), indicating that 25(OH)D_3 does not affect the proliferation of H9N2 in lung tissues.

Compared to the uninfected mice, IL-1β levels were markedly increased in the lungs of the infected mice on days 3, 7, 14 and 21 post-infection, and the peak levels were observed on day 7 (Fig. 12A). The level of TNF-α was also significantly increased in the lungs of the infected mice on days 3 and 7 (Fig. 12 B). However, 25(OH)D_3 did not affect the levels of IL-1β and TNF-α in the infected mice, indicating that 25(OH)D_3 treatment might not alleviate the inflammatory response in the lungs during H9N2 infection.

4. Discussion

Previous studies have shown that some H9N2 virus strains can infect laboratory mice without adaptation, and cause the typical respiratory disease associated with acute lung injury (ALI) [32,36]. In this study, mice infected with 1×10^6 $TCID_{50}$ H9N2 exhibited obvious clinical signs on days 3 and 7 post-infection, including labored respiration, inactivity, lack of appetite and weight loss. Furthermore, the infected lungs exhibited serious edema and hemorrhage on day 7. By day 14 however, the mice had largely recovered and regained weight, and the viruses were completely eliminated from the lungs. The virus dose used in our study simulated the entire pathogenic course from infection to recovery.

In addition to bone mineralization and calcium homeostasis [15], D3 might also play a role in host resistance and immune responses to infection [35]. The immunomodulatory effects of D3 rely on the activation of 25(OH)D_3 and binding with VDR in specific tissues [37]. Therefore, the changes in D3 metabolism enzymes and VDR expression levels during H9N2 infection can better help understand the relationship between vitamin D and influenza.

Cytochrome P450 family 27 subfamily B member 1 (CYP27B1) or 25(OH)D_3 1α-hydroxylase catalyzes the hydroxylation of 25(OH)D_3 to 1, 25$(OH)_2D_3$, which is the rate-limiting step in the synthesis of 1, 25$(OH)_2D_3$ [38]. It is highly expressed in the kidneys [39], followed by keratinocytes [40], intestines [41], breast [42], prostate [43], and immune cells including macrophages [44], monocytes [45] and dendritic cells [46]. In addition, 1α-hydroxylase is upregulated in human tracheobronchial epithelial cells infected with viral RNA or live respiratory syncytial virus *in vitro* [31]. Likewise, 1α-hydroxylase mRNA and protein levels were significantly increased in the lungs of H9N2-infected mice, indicating that the lung tissues had the potential to convert 25(OH)D_3 to 1, 25$(OH)_2D_3$ during H9N2 infection.

D3 exerts its biological effects by regulating gene expression through VDR [37], a transcription factor present in nearly all cells and may be responsible for the extra-skeletal effects of D3 [20]. VDR modulates the expression of several genes, including those involved immune responses, in a cell and tissue-specific manner [47]. VDR-knockout mice show defective macrophage function and cellular immunity *in vitro* and *in vivo* [48]. In the present study, VDR mRNA and protein levels were markedly increased in the lungs of mice infected with H9N2, which suggested that the responsiveness of lung tissue to 1, 25$(OH)_2D_3$ might be enhanced by H9N2 infection.

Vitamin D 24-hydroxylase, also known as cytochrome P450 family 24 subfamily A member 1 (CYP24A1), catalyzes hydroxylation of 1, 25$(OH)_2D_3$ [30]. The latter induces its rapid degradation through a negative feedback loop by upregulating 24-hydroxylase [30]. In the present study, 24-hydroxylase mRNA and protein expression levels were unaffected by H9N2 infection. Taking into account the upregulation of 1α-hydroxylase and VDR, this indicates that the negative feedback loop of D3 is not initiated, which may increase the concentration of active D3 in the lungs. Thus, D3 signaling pathway might be amplified in the lungs during H9N2 infection.

The expression levels of 1α-hydroxylase and VDR are regulated by external stimuli in a tissue-specific manner. Studies show that regulation of 1α-hydroxylase, VDR and 24-hydroxylases in immune cells depend on the tissue or cell type, as well as the differentiation or activation status of the cells. For example, VDR and 1α-hydroxylase are expressed in the activated T-cells [49], monocytes and macrophages [50,51]. H9N2 infection results in excessive pulmonary inflammation, characterized by massive infiltration of immune cell and cytokine production [32], which could explain the increased expression of VDR and 1α-hydroxylase in the lungs of the infected mice. In addition, several recent studies have suggested that D3 deficiency is a risk factor for coronavirus 2019 (COVID-19) infection [52,53]. D3 supplementation might be reasonable for the prevention severe acute respiratory syndrome coronavirus 2 (SARS-CoV-2) infection, and reduce morbidity and mortality in the high-risk patients with vitamin D deficiency [54,55]. Therefore, we recommend detecting the expression levels of D3 metabolic enzymes

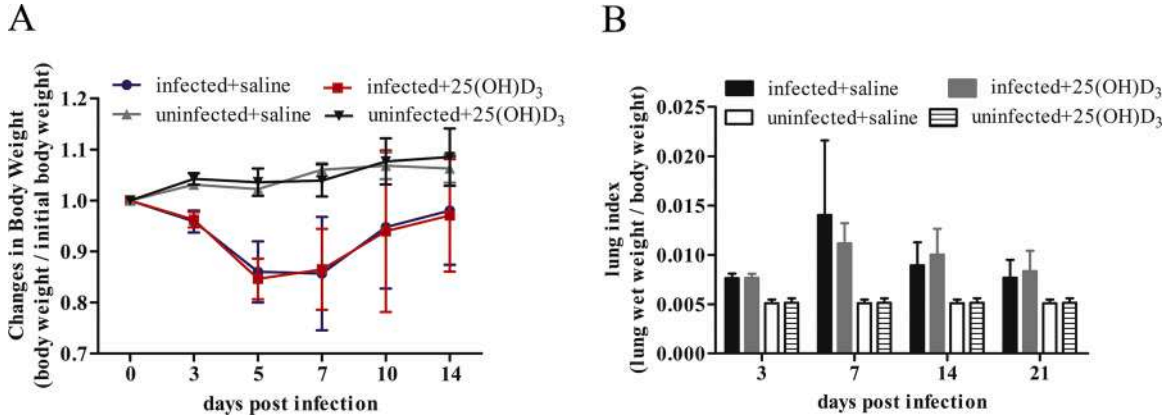

Fig. 9. The body weight and lung indexes of mice after 25(OH)D_3 treatment. Mice were intranasally inoculated with H9N2 viruses, and then were intraperitoneally injected daily with 0.2 mL 25(OH)D_3 solution (4 μg/kg) on days 2 to 14 post-infection. The lung tissues were collected on days 3, 7, 14 and 21 post-infection. (A) The body weight changes of mice. (B) The lung indexes of mice on days 3, 7, 14 and 21. The data were presented as mean ± SD (n = 5). No statistically significant differences were observed in body weight changes and lung indexes at different time points between the 25(OH)D_3-treated and saline-treated mice infected with H9N2 viruses.

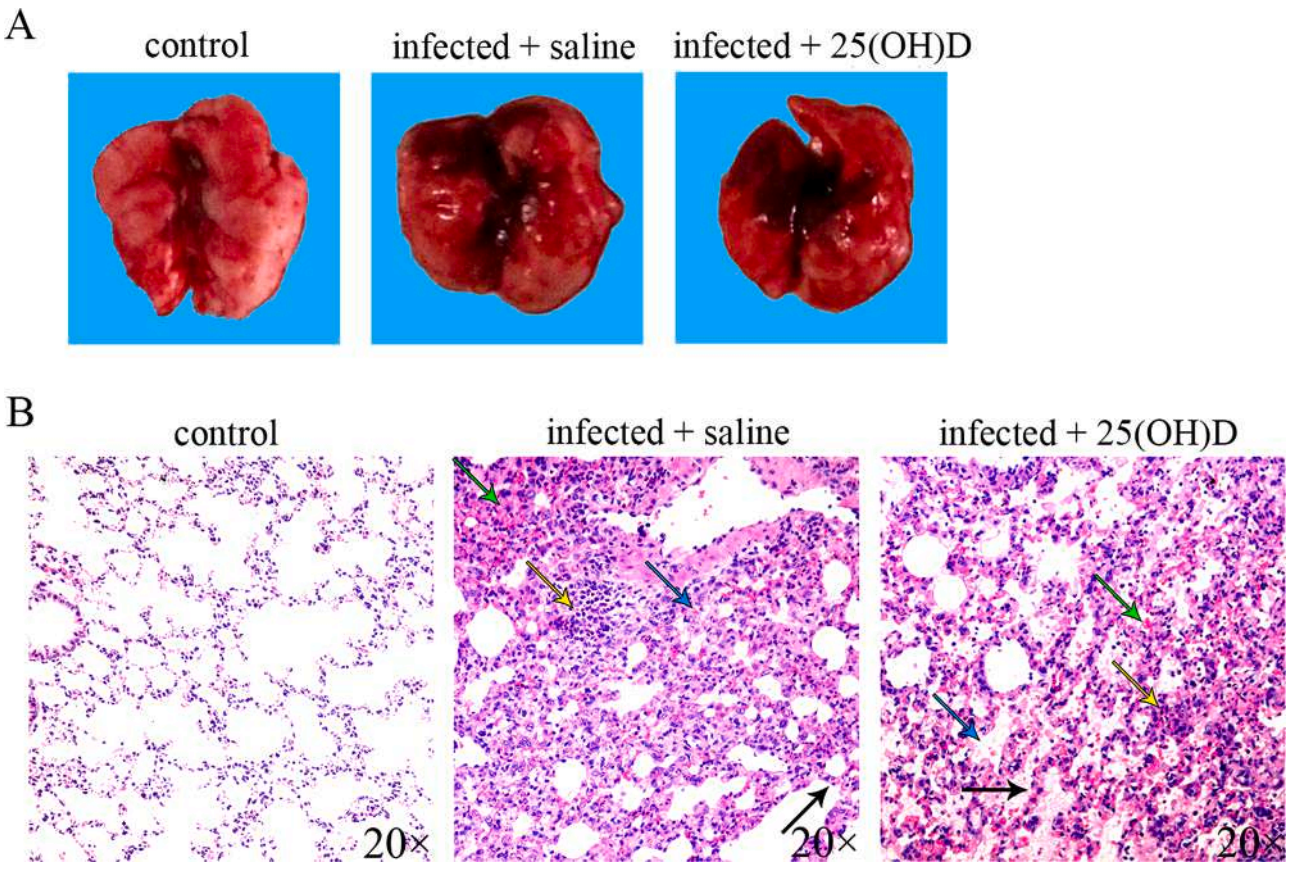

Fig. 10. Lung gross pathology and histopathology of mice after 25(OH)D_3 treatment. Mice were intranasally inoculated with H9N2 viruses, and then were intraperitoneally injected daily with 0.2 mL 25(OH)D_3 solution (4 μg/kg) on days 2 to 14 post-infection. The lung tissues were collected on day 7 post-infection. (A) Lungs gross pathology of mice on day 7 post-infection. The 25(OH)D_3-treated and saline-treated infected mice lungs showed similar degree of injury, including edema and hemorrhage. (B) Lungs histopathology of mice on day 7 post-infection. Thickening of the alveolar wall (black arrows), severe edema (blue arrows), hemorrhage (green arrows) and inflammatory cellular infiltration (yellow arrows) were observed in lungs of infected mice. The lungs histopathological pattern observed in 25 (OH)D_3-treated infected mice was similar to that in saline-treated infected mice.

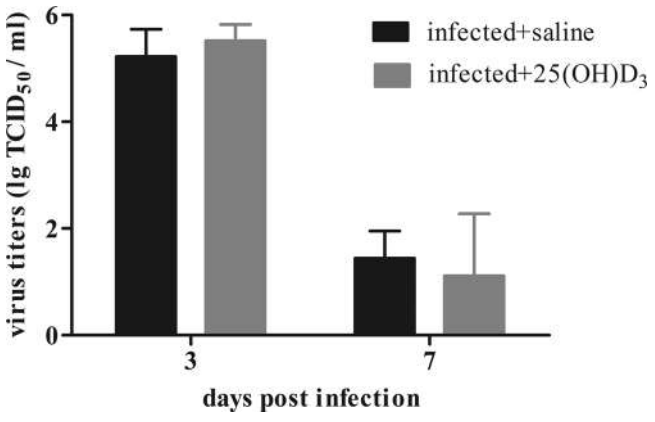

Fig. 11. Replication of H9N2 viruses in lungs of mice after 25(OH)D_3 treatment. Mice were intranasally inoculated with H9N2 viruses, and then were intraperitoneally injected daily with 0.2 mL 25(OH)D_3 solution (4 μg/kg) on days 2 to 14 post-infection. The lung tissues were collected on days 3 and 7 post-infection. The viral titers were measured by $TCID_{50}$ assay. Mean viral titers are expressed as $\log_{10}$ $TCID_{50}$ per milliliter ± SD (n = 5). No statistically significant differences were observed in vital titers on days 3 and 7 between the 25 (OH)D_3-treated and saline-treated mice after infection.

and VDR in the target organs before initiating D3 treatment.

The high expressions of 1α-hydroxylase and VDR in the lung tissues mean that D3 signaling pathway might be active during H9N2 viral infection. Studies show that D3 suppresses the inflammatory response by reducing production of pro-inflammatory cytokines [21,24,47]. Excessive cytokine production, also known as cytokine storm, is the underlying cause of the acute lung injury induced by influenza viral infection [56]. In the present study, 25(OH)D_3 treatment did not alleviate the clinical signs of H9N2 infection, and had no effect on the lung indices, virus titers, or the levels of IL-1β and TNF-α in the lung homogenates. Consistent with our findings, Gui et al. showed that daily treatment with 1, 25$(OH)_2D_3$ following H9N2 viral infection did not affect the clinical signs and viral clearance in mice [57]. Furthermore, Khare et al. showed that treatment with 100/30 nM 1, 25$(OH)_2D_3$ before or after H1N1 infection did not affect viral clearance from A549 cells *in vitro*, and 1,25 $(OH)_2D_3$ suppressed viral replication only at the un-physiological dose of 1000 nM [24].

In conclusion, we have shown for the first time that the vitamin D receptor and its activating enzyme (1α-hydroxylase) are significantly upregulated in the lungs of mice infected with H9N2 virus. The nonclassical effects of D3 rely on the D3 signaling pathway, including activation of 25(OH)D_3 and its combination with VDR in specific tissues. Our findings suggest that the D3 signaling pathway is likely activated in the lungs during H9N2 infection, which might contribute to a better understanding of the association between VD and influenza. Although we found that 25(OH)D_3 treatment had little effect on H9N2 infection, it is worth examining the role of D3 in influenza in future studies.

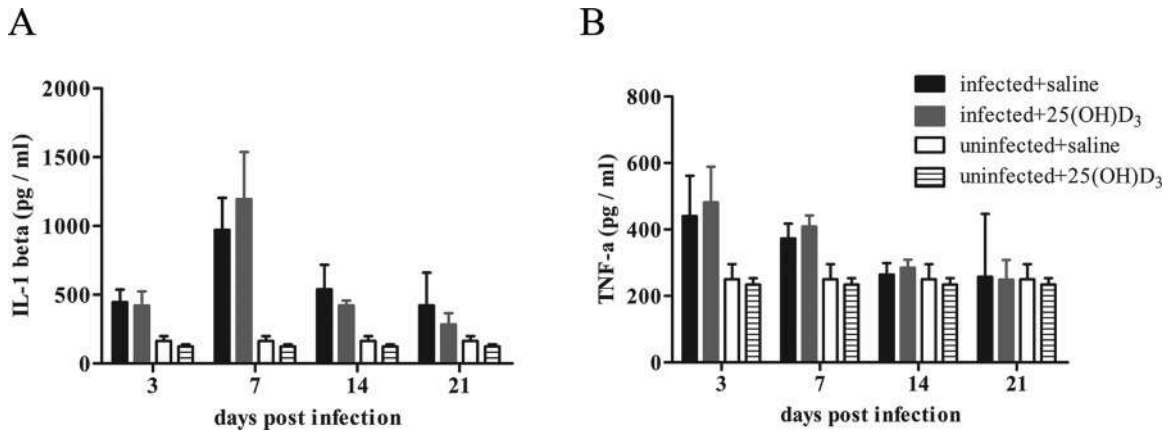

Fig. 12. The levels of IL-1β (A) and TNF-α (B) in lungs of mice after 25(OH)D_3 treatment. Mice were intranasally inoculated with H9N2 viruses, and then were intraperitoneally injected daily with 0.2 mL 25(OH)D_3 solution (4 μg/kg) on days 2 to 14 post-infection. The lung tissues were collected on days 3, 7, 14 and 21 post-infection. The levels of IL-1β and TNF-α in lungs were measured by ELISA assay. The data were presented as mean ± SD (n = 5). No statistically significant differences were observed in the levels of IL-1β and TNF-α at different time points between the 25(OH)D_3-treated and saline-treated mice after infection.

Funding

This work was supported by the national key research and development program: Study on nutrition metabolism and prevention and control technology of toxic diseases of livestock and poultry (No. 2016YFD0501200) and Earmarked Fund for Layer and Broiler Innovation Team of the Second Phase of Hebei Modern Industrial System (HBCT2018150101 and HBCT2018150207).

Declaration of Competing Interest

The authors report no declarations of interest.

Acknowledgements

We thank associate professor Yanxin Hu for assistance with H&E staining of lung tissues. We thank associate professor Tianlong Liu for supplying the instrument and equipment for our experiments. Both associate professor Hu and Liu are affliated with the Department of Pathology, College of Veterinary Medicine, China Agricultural University, Beijing, China

References

[1] Y. Sun, J. Liu, H9N2 influenza virus in China: a cause of concern, Protein Cell 6 (2015) 18–25.
[2] Y. Cong, C. Wang, C. Yan, J.-S. Peng, Z.-L. Jiang, J.-H. Liu, Swine infection with H9N2 influenza viruses in China in 2004, Virus Genes 36 (2008) 461.
[3] X. Sun, X. Xu, Q. Liu, D. Liang, C. Li, Q. He, et al., Evidence of avian-like H9N2 influenza A virus among dogs in Guangxi, China, Infect. Genet. Evol. 20 (2013) 471–475.
[4] Y. Guo, J. Li, X. Cheng, [Discovery of men infected by avian influenza A (H9N2) virus], Zhonghua Shi Yan He Lin Chuang Bing Du Xue Za Zhi 13 (1999) 105–108.
[5] T. Saito, W. Lim, T. Suzuki, Y. Suzuki, H. Kida, S.I. Nishimura, et al., Characterization of a human H9N2 influenza virus isolated in Hong Kong, Vaccine 20 (2001) 125–133.
[6] W. Song, K. Qin, Human-infecting influenza A (H9N2) virus: a forgotten potential pandemic strain? Zoonoses Public Health 67 (2020) 203–212.
[7] K. Subbarao, X. Li, J. Shi, J. Guo, G. Deng, Q. Zhang, et al., Genetics, receptor binding property, and transmissibility in mammals of naturally isolated H9N2 avian influenza viruses, PLoS Pathog. (2014) 10.
[8] Chang H-p, L. Peng, L. Chen, Jiang L-f, Zhang Z-j, Xiong C-l, et al., Avian influenza viruses (AIVs) H9N2 are in the course of reassorting into novel AIVs, J. Zhejiang Univ.-Sci. B 19 (2018) 409–414.
[9] Y. Guan, K. Shortridge, S. Krauss, R. Webster, Molecular characterization of H9N2 influenza viruses: were they the donors of the "internal" genes of H5N1 viruses in Hong Kong? Proc. Natl. Acad. Sci. U. S. A. 96 (1999) 9363–9367.
[10] R. Gao, B. Cao, Y. Hu, Z. Feng, D. Wang, W. Hu, et al., Human infection with a novel avian-origin influenza A (H7N9) virus, N. Engl. J. Med. 368 (2013) 1888–1897.
[11] H. Chen, H. Yuan, R. Gao, J. Zhang, D. Wang, Y. Xiong, et al., Clinical and epidemiological characteristics of a fatal case of avian influenza A H10N8 virus infection: a descriptive study, Lancet 383 (2014) 714–721.
[12] Y. Bi, Q. Chen, Q. Wang, J. Chen, T. Jin, G. Wong, et al., Genesis, evolution and prevalence of H5N6 avian influenza viruses in China, Cell Host Microbe 20 (2016) 810–821.
[13] J.J. Cannell, R. Vieth, J.C. Umhau, M.F. Holick, W.B. Grant, S. Madronich, et al., Epidemic influenza and vitamin D, Epidemiol. Infect. 134 (2006) 1129–1140.
[14] R.E. Hope-Simpson, The role of season in the epidemiology of influenza, J. Hyg. (Lond.) 86 (1981) 35–47.
[15] J.S. Adams, M. Hewison, Update in vitamin D, J. Clin. Endocrinol. Metab. 95 (2010) 471–478.
[16] N.S. Akimbekov, R.A. Ortoski, M.S. Razzaque, Effects of sunlight exposure and vitamin D supplementation on HIV patients, J. Steroid Biochem. Mol. Biol. 200 (2020), 105664.
[17] J. Moan, A. Dahlback, L. Ma, A. Juzeniene, Influenza, solar radiation and vitamin D, Dermatoendocrinology 1 (2009) 307–309.
[18] J. Shaman, C.Y. Jeon, E. Giovannucci, M. Lipsitch, Shortcomings of vitamin D-based model simulations of seasonal influenza, PLoS One 6 (2011), e20743.
[19] P. Lips, Vitamin d physiology, Prog. Biophys. Mol. Biol. 92 (2006) 4–8.
[20] D.D. Bikle, Extraskeletal actions of vitamin D, Ann. N. Y. Acad. Sci. 1376 (2016) 29–52.
[21] F. Baeke, T. Takiishi, H. Korf, C. Gysemans, C. Mathieu, Vitamin D: modulator of the immune system, Curr. Opin. Pharmacol. 10 (2010) 482–496.
[22] P.T. Liu, S. Stenger, D.H. Tang, R.L. Modlin, Cutting edge: vitamin D-mediated human antimicrobial activity against Mycobacterium tuberculosis is dependent on the induction of cathelicidin, J. Immunol. 179 (2007) 2060–2063.
[23] J.S. Adams, S. Ren, P.T. Liu, R.F. Chun, V. Lagishetty, A.F. Gombart, et al., Vitamin d-directed rheostatic regulation of monocyte antibacterial responses, J. Immunol. 182 (2009) 4289–4295.
[24] S. Hansdottir, M.M. Monick, N. Lovan, L. Powers, A. Gerke, G.W. Hunninghake, Vitamin D decreases respiratory syncytial virus induction of NF-kappaB-linked chemokines and cytokines in airway epithelium while maintaining the antiviral state, J. Immunol. 184 (2010) 965–974.
[25] D. Khare, N.M. Godbole, S.D. Pawar, V. Mohan, G. Pandey, S. Gupta, et al., Calcitriol [1, 25[OH]2 D3] pre- and post-treatment suppresses inflammatory response to influenza A (H1N1) infection in human lung A549 epithelial cells, Eur. J. Nutr. 52 (2013) 1405–1415.
[26] A.T. Slominski, T.K. Kim, W. Li, A. Postlethwaite, E.W. Tieu, E.K.Y. Tang, et al., Detection of novel CYP11A1-derived secosteroids in the human epidermis and serum and pig adrenal gland, Sci. Rep. 5 (2015) 14875.
[27] A.T. Slominski, T.K. Kim, H.Z. Shehabi, I. Semak, E.K. Tang, M.N. Nguyen, et al., In vivo evidence for a novel pathway of vitamin D(3) metabolism initiated by P450scc and modified by CYP27B1, FASEB J. 26 (2012) 3901–3915.
[28] A.T. Slominski, T.K. Kim, Y. Takeda, Z. Janjetovic, A.A. Brozyna, C. Skobowiat, et al., RORalpha and ROR gamma are expressed in human skin and serve as receptors for endogenously produced noncalcemic 20-hydroxy- and 20,23-dihydroxyvitamin D, FASEB J. 28 (2014) 2775–2789.
[29] R. Shinde, T.L. McGaha, The aryl hydrocarbon receptor: connecting immunity to the microenvironment, Trends Immunol. 39 (2018) 1005–1020.
[30] G. Jones, D.E. Prosser, M. Kaufmann, 25-Hydroxyvitamin D-24-hydroxylase (CYP24A1): its important role in the degradation of vitamin D, Arch. Biochem. Biophys. 523 (2012) 9–18.
[31] S. Hansdottir, M.M. Monick, S.L. Hinde, N. Lovan, D.C. Look, G.W. Hunninghake, Respiratory epithelial cells convert inactive vitamin D to its active form: potential effects on host defense, J. Immunol. 181 (2008) 7090–7099.
[32] G. Deng, J. Bi, F. Kong, X. Li, Q. Xu, J. Dong, et al., Acute respiratory distress syndrome induced by H9N2 virus in mice, Arch. Virol. 155 (2010) 187–195.

[33] J. Bi, G. Deng, J. Dong, F. Kong, X. Li, Q. Xu, et al., Phylogenetic and molecular characterization of H9N2 influenza isolates from chickens in Northern China from 2007-2009, PLoS One (2010) 5.
[34] V.J. Munster, E. de Wit, J.M. van den Brand, S. Herfst, E.J. Schrauwen, T. M. Bestebroer, et al., Pathogenesis and transmission of swine-origin 2009 A(H1N1) influenza virus in ferrets, Science 325 (2009) 481–483.
[35] J.A. Beard, A. Bearden, R. Striker, Vitamin D and the anti-viral state, J. Clin. Virol. 50 (2011) 194–200.
[36] Y.J. Guo, S. Krauss, D.A. Senne, I.P. Mo, K.S. Lo, X.P. Xiong, et al., Characterization of the pathogenicity of members of the newly established H9N2 influenza virus lineages in Asia, Virology 267 (2000) 279–288.
[37] M.R. Haussler, P.W. Jurutka, M. Mizwicki, A.W. Norman, Vitamin D receptor (VDR)-mediated actions of 1α,25(OH)2vitamin D3: Genomic and non-genomic mechanisms, Best Pract. Res. Clin. Endocrinol. Metab. 25 (2011) 543–559.
[38] H.F. DeLuca, Overview of general physiologic features and functions of vitamin D, Am. J. Clin. Nutr. 80 (2004) 1689s–1696s.
[39] D.R. Fraser, E. Kodicek, Unique biosynthesis by kidney of a biological active vitamin D metabolite, Nature 228 (1970) 764–766.
[40] D.D. Bikle, M.K. Nemanic, E. Gee, P. Elias, 1,25-Dihydroxyvitamin D3 production by human keratinocytes. Kinetics and regulation, J. Clin. Invest. 78 (1986) 557–566.
[41] B.W. Ogunkolade, B.J. Boucher, P.D. Fairclough, G.A. Hitman, S. Dorudi, P. J. Jenkins, et al., Expression of 25-hydroxyvitamin D-1-alpha-hydroxylase mRNA in individuals with colorectal cancer, Lancet 359 (2002) 1831–1832.
[42] C.M. Kemmis, S.M. Salvador, K.M. Smith, J. Welsh, Human mammary epithelial cells express CYP27B1 and are growth inhibited by 25-hydroxyvitamin D-3, the major circulating form of vitamin D-3, J. Nutr. 136 (2006) 887–892.
[43] G.G. Schwartz, L.W. Whitlatch, T.C. Chen, B.L. Lokeshwar, M.F. Holick, Human prostate cells synthesize 1,25-dihydroxyvitamin D3 from 25-hydroxyvitamin D3, Cancer Epidemiol. Biomark. Prev. 7 (1998) 391–395.
[44] J.S. Adams, M.A. Gacad, F.R. Singer, O.P. Sharma, Production of 1,25-dihydroxy-vitamin D3 by pulmonary alveolar macrophages from patients with sarcoidosis, Ann. N. Y. Acad. Sci. 465 (1986) 587–594.
[45] M. Kreutz, R. Andreesen, S.W. Krause, A. Szabo, E. Ritz, H. Reichel, 1,25-dihydroxyvitamin D3 production and vitamin D3 receptor expression are developmentally regulated during differentiation of human monocytes into macrophages, Blood 82 (1993) 1300–1307.
[46] H. Sigmundsdottir, J. Pan, G.F. Debes, C. Alt, A. Habtezion, D. Soler, et al., DCs metabolize sunlight-induced vitamin D3 to' program' T cell attraction to the epidermal chemokine CCL27, Nat. Immunol. 8 (2007) 285–293.
[47] R. Rezaei, S. Aslani, M. Marashi, F. Rezaei, E. Sharif-Paghaleh, Immunomodulatory effects of vitamin D in influenza infection, Curr. Immunol. Rev. 14 (2018) 40–49.
[48] C. Mathieu, E. Van Etten, C. Gysemans, B. Decallonne, S. Kato, J. Laureys, et al., In vitro and in vivo analysis of the immune system of vitamin D receptor knockout mice, J. Bone Miner. Res. 16 (2001) 2057–2065.
[49] K. Edfeldt, P.T. Liu, R. Chun, M. Fabri, M. Schenk, M. Wheelwright, et al., T-cell cytokines differentially control human monocyte antimicrobial responses by regulating vitamin D metabolism, Proc. Natl. Acad. Sci. U. S. A. 107 (2010) 22593–22598.
[50] K. Stoffels, L. Overbergh, A. Giulietti, L. Verlinden, R. Bouillon, C. Mathieu, Immune regulation of 25-hydroxyvitamin-D3-1alpha-hydroxylase in human monocytes, J. Bone Miner. Res. 21 (2006) 37–47.
[51] Y. Wang, J. Zhu, H.F. DeLuca, Where is the vitamin D receptor? Arch. Biochem. Biophys. 523 (2012) 123–133.
[52] R.M. Slominski, J. Stefan, M. Athar, M.F. Holick, A.M. Jetten, C. Raman, et al., COVID-19 and vitamin D: a lesson from the skin, Exp. Dermatol. 29 (2020) 885–890.
[53] E.K. Weir, T. Thenappan, M. Bhargava, Y. Chen, Does vitamin D deficiency increase the severity of COVID-19? Clin. Med. (Lond) 20 (2020) e107–e108.
[54] A. Bleizgys, Vitamin D and COVID-19: It is time to act, Int. J. Clin. Pract. (2020), e13748.
[55] D. Siuka, M. Pfeifer, B. Pinter, Vitamin d supplementation during the COVID-19 pandemic, Mayo Clin. Proc. 95 (2020) 1804–1805.
[56] M. Bhatia, S. Moochhala, Role of inflammatory mediators in the pathophysiology of acute respiratory distress syndrome, J. Pathol. 202 (2004) 145–156.
[57] B. Gui, Q. Chen, C. Hu, C. Zhu, G. He, Effects of calcitriol (1, 25-dihydroxy-vitamin D3) on the inflammatory response induced by H9N2 influenza virus infection in human lung A549 epithelial cells and in mice, Virol. J. 14 (2017) 10.